**Structural Engineering and Mechanics**, *Vol. 54, No. 6 (2015) 1045-1059*
DOI: http://dx.doi.org/10.12989/sem.2015.54.6.1045 

# Modified nonlinear force density method for form-finding of membrane SAR antenna

Rui Xu[a], DongXu Li*, Wang Liu[b], JianPing Jiang[c], YiHuan Liao[d] and Jie Wang[e]

*College of Aerospace Science and Engineering, National University of Defense Technology, Changsha, Hunan, 410073, People's Republic of China*

*(Received September 11, 2014, Revised January 4, 2015, Accepted January 23, 2015)*

**Abstract.** Form-finding for cable-membrane structures is a delicate operation. During the last decades, the force density method (FDM) was considered to be an efficient method to address the problem. Many researchers were devoted to improving this method and proposed many methods such as natural force density method (NFDM), improved nonlinear force density method (INFDM), et al. In this paper, a modified nonlinear force density method (MNFDM) is proposed. In this method, the stresses of membrane elements were transformed to the force-densities of cable nets by an equivalent relationship, and then they can be used as initial conditions. By comparing with the forming finding results by using the FDM, NFDM, INFDM and MNFDM, it had demonstrated that the MNFDM presented in this paper is the most efficient and precise.

**Keywords:** form-finding; cable-membrane structure; force density method (FDM); equivalent transform relationship

## 1. Introduction

Cable-membrane structures have a very attractive characteristic of large span distances. They are expected to be very light, elegant, and efficient (Bradshaw *et al*. 2002). These advantages make cable-membrane structures play a major role in engineering practice. Nowadays, cable-membrane structures have gained wide applications in space missions, such as spaceborne membrane SAR antenna. JPL (Grahne and Cadogan 1999), DLR (Straubel *et al*. 2010) and CSA (Colinas *et al*. 2005) have been performed their efforts on the development of membrane SAR antenna program, respectively. The membrane SAR antenna is typically composed of three components, the support

*Corresponding author, Professor, E-mail: dongxuli@nudt.edu.cn
[a]Ph.D. Student, E-mail: xurui@nudt.edu.cn
[b]Ph.D., E-mail: wangliu@nudt.edu.cn
[c]Ph.D., E-mail: jianping202@163.com
[d]Ph.D., E-mail: liaoyihuan@hotmail.com
[e]Ph.D. Student, E-mail: willianmking@yeah.net


http://www.techno-press.org/?journal=sem&subpage=8 ISSN: 1225-4568 (Print), 1598-6217 (Online)

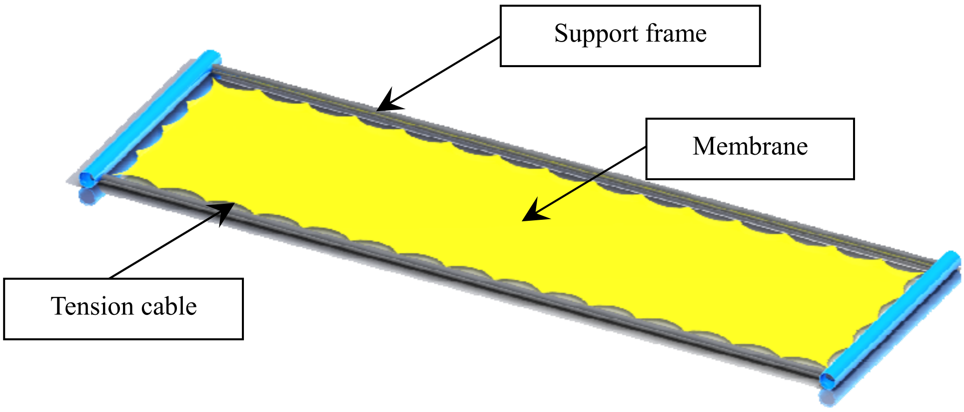


Fig. 1 The membrane SAR antenna

frame, tension cable and the membrane as showed in Fig. 1. The membrane is ultra-thin, lightweight and of extremely large size (several hundred square meters) (Lane *et al*. 2011), and has high surface flatness requirement (less than 5 mm). Tensioning the membrane is an effective method to render it flat. The experiments proposed by Leifer *et al*. (2010) indicate that the increasing the tautness of the membrane significantly reduces (but does not eliminate) the surface wrinkling. If the tension stress in the membrane is distributed well, it will make more efforts on increasing the surface flatness. Hence, design a uniform tension stress field in the membrane is expect necessary.

For cable-membrane structures, the stresses distribution in it is a direct result of the structural shape. Therefore, the self-equilibrium shape should be decided by a form-finding analysis that simultaneously gets the feasible set of internal stresses distribution and geometry of the structure (Ye *et al*. 2012). It is a fundamental step in the design of a membrane SAR antenna. Up to now, there are various techniques having been proposed to solve the form finding problem, such as Force Density Method (FDM) (Zhang *et al*. 2007, Pauletti and Pimenta 2008, Ye *et al*. 2012), Dynamic Relaxation Method (DRM) (Barnes 1999, Zhang *et al*. 2006, Xu and Luo 2011), geometrically nonlinear finite element method (Valdés *et al*. 2009), minimal surface method (Tsiatas and Katsikadelis 2006). Veenendaal and Block (2012) have discussed and compared these form finding methods and presented a single computational framework. DRM starting from an arbitrary non equilibrated configuration the final form is resolved by means of an iterative pseudo-dynamical process, with each iteration based on an update of the geometry (Greco and Cuomo 2012). However, DRM requires too many parameters, such as time step, to control stability and convergence (Nouri-Baranger 2004), and resents of dynamic stability problems.

FDM is originally proposed by Linkwitz (1971a, b), Scheck (1974), and its main feature lies in prescribing a force density, namely the ratio of force-to-length, for each cable element. This method was first developed to solve the form finding problem of cable networks, and was used to find the form of double layer grid structure (Tran and Lee 2013), slack cable nets (Greco and Cuomo 2012), flexible bridge decks (Quagliaroli and Malerba 2013) and cable net antennas (Hernandez-Montes *et al*. 2006, Morterolle *et al*. 2012, Liu *et al*. 2013a, b, c). Then Maurin and Motro (1998) introduced it into shape finding problem of membrane structures and proposed some analogous procedures. When applying the FDM to cable-membrane structures, the structure is first modeled as cable nets, thus the FDM can convert the nonlinear problem into linear equations that can be readily solved. FDM is an attractive method, and it has universal applicability and advantages. However, FDM had not considered the variety of the cable member length. In order to preserve the linearity of the original force density method and retains its simplicity and robustness, Pauletti and Pimenta (2008) propose the natural force density method (NFDM). The stress field is calculated by updating the reference configuration and then the desired stress field. As the width of the member element is also varying in the form finding process, Xiang *et al*. (2010) presented an improved nonlinear force density method (INFDM) taking into account of the effect of 2-dimensional deformations of the membrane surface. However, in all these methods, the force density can only be determined after several trial calculations, which often is dependent on the experience of the researchers. Moreover, stresses distribution in the membrane is hard to assess, especially for membrane structures with flexible boundaries (Maurin and Motro 1998, 2004, Ye *et al*. 2012). The stresses distribution of the form-finding shape will not agree with the given design stresses distribution.

In this paper, a modified nonlinear force density method (MNFDM) is proposed. The disadvantages of the above-mentioned methods were addressed through the following modification: the stresses of membrane elements were transformed to the force-densities of cable nets by an equivalent relationship. With this transformation the form-finding of the membrane structures will be of high efficiency. Membrane stresses and cable tension can be introduced as initial conditions to establish a quantitative relationship between the force densities and the internal forces of the structure, which would avoid the complicated trial calculation process and simplify the form finding computation for the cable-membrane structures.

## 2. An outline of the force density method

In order to apply FDM to cable-membrane structure, first, the membrane is discretized into elements and modeled as a cable net. Consider a cable net has $n$ free nodes and $n_f$ fixed nodes, connected by $m$ elements. The total number of nodes is $n_s$=$n$+$n_f$. With reference to the $i$th node of a 3D net (Fig. 2), the equilibrium equations in the $x$, $y$, $z$ directions are respectively

$$\begin{cases} T_{ij}\dfrac{x_j-x_i}{L_{ij}}+T_{ik}\dfrac{x_k-x_i}{L_{ik}}+T_{il}\dfrac{x_l-x_i}{L_{il}}+T_{im}\dfrac{x_m-x_i}{L_{im}}+F_{xi}=0 \\ T_{ij}\dfrac{y_j-y_i}{L_{ij}}+T_{ik}\dfrac{y_k-y_i}{L_{ik}}+T_{il}\dfrac{y_l-y_i}{L_{il}}+T_{im}\dfrac{y_m-y_i}{L_{im}}+F_{yi}=0 \\ T_{ij}\dfrac{z_j-z_i}{L_{ij}}+T_{ik}\dfrac{z_k-z_i}{L_{ik}}+T_{il}\dfrac{z_l-z_i}{L_{il}}+T_{im}\dfrac{z_m-z_i}{L_{im}}+F_{zi}=0 \end{cases} \tag{1}$$

where $T_{ij}$ is the axial force and $L_{ij}$ is the length of the element between the nodes $i$ and $j$

$$L_{ij}=\sqrt{\left(x_i-x_j\right)^2+\left(y_i-y_j\right)^2+\left(z_i-z_j\right)^2} \tag{2}$$

Suppose that the topology of the cable net structure is known at the start of the analysis. The member-node incidence matrix, also called structural topological matrix, which describes the connectivity of the cable members to the nodes, are given by

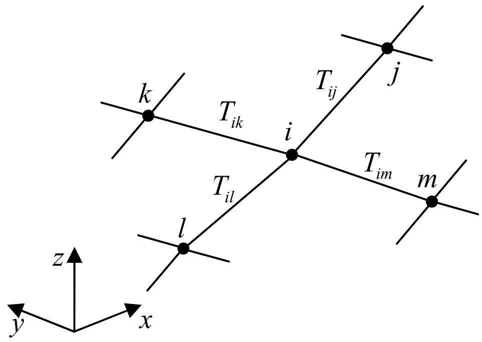


Fig. 2 Generically free node

$$\boldsymbol{C}_s(p,q)=\begin{cases}+1 & \text{if } q=i\\ -1 & \text{if } q=j\\ 0 & \text{for other cases}\end{cases} \tag{3}$$

where $p$ is the row number of matrix $\mathbf{C}_s$ denotes the $p$-th cable member that matches node $i$ and node $j$ ($i<j$), $\mathbf{C}_s$ is an $m$ by $n_s$ matrix.

For convenience of subsequent analysis, by partitioning the matrix $\mathbf{C}_s$, we can put in evidence separately the coordinates of the free and those of the fixed nodes, as follows

$$\boldsymbol{C}_s=\begin{bmatrix}\boldsymbol{C}_u & \boldsymbol{C}_f\end{bmatrix} \tag{4}$$

where $\mathbf{C}_u \in \mathrm{R}^{m\times n}$ and $\mathbf{C}_f \in \mathrm{R}^{m\times n_f}$ describe the connectivity of the members to the free and fixed nodes, respectively.

Take $x$-direction for instance, the projection of the cable member on $x$-axis is

$$\boldsymbol{u}=\boldsymbol{C}_s\boldsymbol{x}_s=\boldsymbol{C}_u\boldsymbol{x}_u+\boldsymbol{C}_f\boldsymbol{x}_f \tag{5}$$

where $x_s$, $x_f$ and $x$ are $x$ coordinates of the total nodes, free nodes and fixed nodes, respectively.

Introduce the concept of force density $q_{ij}=T_{ij}/L_{ij}$, denote $\mathbf{q}$ is the force densities of the members, $\mathbf{Q}$=*diag*($\mathbf{q}$). Then the equilibrium equations of the cable net can be set out into a matrix form

$$\boldsymbol{C}_s^T\mathbf{Q}\mathbf{C}_s\mathbf{x}_s=\mathbf{p}_{xs} \tag{6}$$

Generally

$$\begin{bmatrix}\mathbf{C}^T\\ \mathbf{C}_f^T\end{bmatrix}\mathbf{Q}\begin{bmatrix}\mathbf{C} & \mathbf{C}_f\end{bmatrix}\begin{Bmatrix}\mathbf{x}\\ \mathbf{x}_f\end{Bmatrix}=\begin{Bmatrix}\mathbf{p}_x\\ \mathbf{p}_{xf}\end{Bmatrix} \tag{7}$$

Then

$$\begin{cases}\mathbf{C}^T\mathbf{Q}\mathbf{C}\mathbf{x}+\mathbf{C}^T\mathbf{Q}\mathbf{C}_f\mathbf{x}_f=\mathbf{p}_x\\ \mathbf{C}_f^T\mathbf{Q}\mathbf{C}\mathbf{x}+\mathbf{C}_f^T\mathbf{Q}\mathbf{C}_f\mathbf{x}_f=\mathbf{p}_{xf}\end{cases} \tag{8}$$

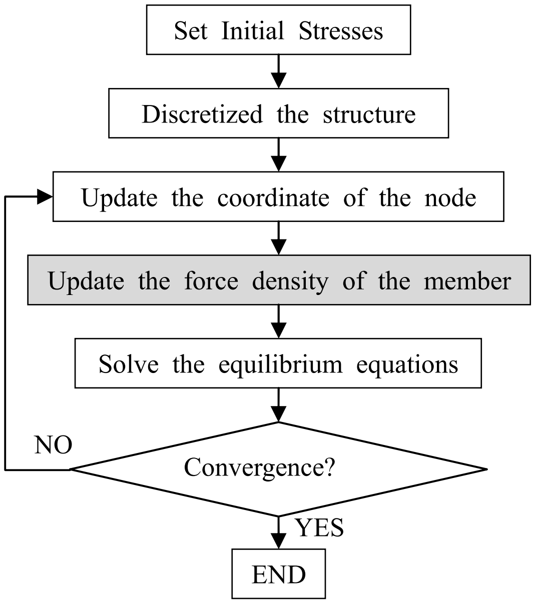


Fig. 3 The flow chart of the NFDM

Letting $\mathbf{D}=\mathbf{C}^T\mathbf{QC}$ and $\mathbf{D}_f=\mathbf{C}^T\mathbf{QC}_f$, we have finally

$$\mathbf{x}=\mathbf{D}^{-1}\left(\mathbf{p}_x-\mathbf{D}_f\mathbf{x}_f\right) \tag{9}$$

The above provides the equations of FDM. In these equations, the force density $\mathbf{q}$ is constant, but the member length $L$ is variation, this will makes the tension force $T=q\times L$ did not match the initial value. In order to overcome this disadvantage, the NFDM use the viable configuration as reference configuration, in which the force density is updated by $q_{i+1}=T/L_i$ ($i$ is the iteration number, $T$ is keeping fixed) in every iteration. The flow chart of NFDM is illustrated in Fig. 3. First the initial stresses are set, and the structure is discretized. Then the coordinate of the node and the force density of the member are updated. After that, the equilibrium equations displayed in Eq. (6) are solved. If the unbalance force error is less than a set value, the form finding process could be ended. Otherwise, the program will run one more loop. In INFDM, the force density of the membrane member updated by $q_{i+1}=s\cdot W_i/L_i$, where $s$ and $W$ are the stresses and width of the membrane elements, respectively. In this paper, the force densities of the membrane member will be updated according to an equilibrium transformation relationship, which will lead to a more accurate solution.

## 3. Equivalent transformation relationship for cables and quadrangle elements

As the elements with a higher number of nodes could result in higher accuracy. In order to reach a higher accuracy, quadrangle element is chosen to discretize the membrane. Consider a planar mesh, with no shear stresses involved, the mesh lines of the elements can be taken as the cable segments of a cable net. The boundary cable segments belongs to one quadrangle membrane

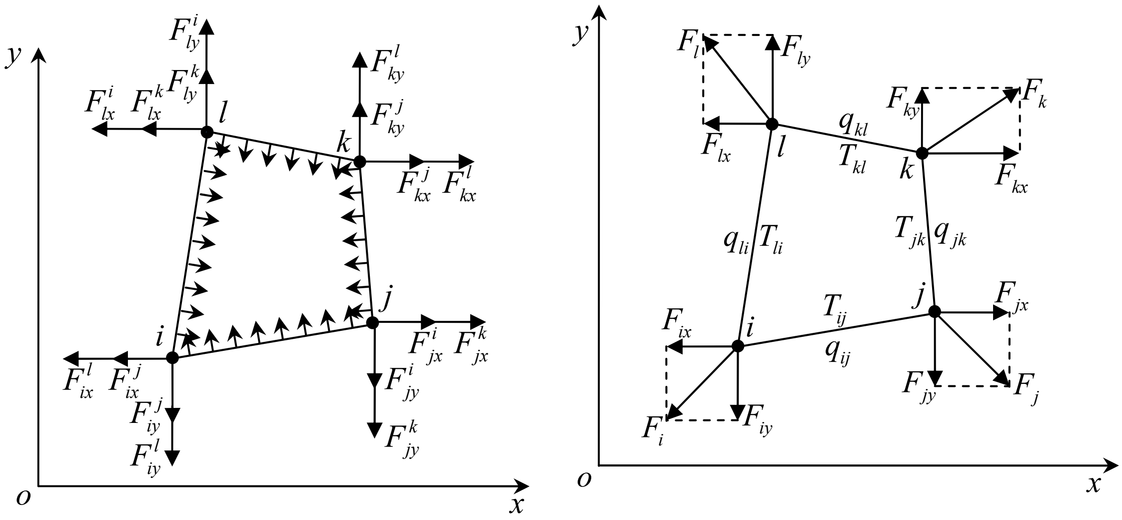

(a) (b)

Fig. 4 Forces of cables and its equivalent nodal force in a single quadrangle element

elements and one cable elements, the other belongs to two quadrangle membrane elements. One of the quadrangle elements is shown in Fig. 4. Denote $\mathbf{T}^e=[T_{ij}\ T_{jk}\ T_{kl}\ T_{li}]^T$ as the force vector and $\mathbf{q}^e=[q_{ij}\ q_{jk}\ q_{kl}\ q_{li}]^T$ as the corresponding force density vector of cables respectively, where $q_{ij}=T_{ij}/L_{ij}$ and $L_{ij}$ is the length of the cables. Denote $\mathbf{F}^e=[F_i\ F_j\ F_k\ F_l]^T$ as the equivalent nodal force vector, and $\mathbf{F}_x^e=\begin{bmatrix}F_{ix} & F_{jx} & F_{kx} & F_{lx}\end{bmatrix}^T$ $\mathbf{F}_y^e=\begin{bmatrix}F_{iy} & F_{jy} & F_{ky} & F_{ly}\end{bmatrix}^T$

Under the above assumption of straight cable members, the cable member can be treated as a tension truss structure. Consequently, the equilibrium equation of cable member $ij$ is

$$F_{ix}^j = F_{jx}^i = \frac{1}{2}\sigma_{ij} t L_{ij}\sin\theta_{ij} = \frac{1}{2}\sigma_x t\left(y_j - y_i\right) \tag{10}$$

$$F_{iy}^j = F_{jy}^i = \frac{1}{2}\sigma_{ij} t L_{ij}\cos\theta_{ij} = \frac{1}{2}\sigma_y t\left(x_j - x_i\right) \tag{11}$$

Similarly, the equilibrium equation of cable member $li$ is

$$F_{ix}^l = F_{lx}^i = \frac{1}{2}\sigma_{li} t L_{li}\sin\theta_{li} = \frac{1}{2}\sigma_x t\left(y_i - y_l\right) \tag{12}$$

$$F_{iy}^l = F_{ly}^i = \frac{1}{2}\sigma_{li} t L_{li}\cos\theta_{li} = \frac{1}{2}\sigma_y t\left(x_i - x_l\right) \tag{13}$$

Hence, the node force of node $i$ is

$$F_{ix} = F_{ix}^j + F_{ix}^l = \frac{1}{2}\sigma_x t\left(y_j - y_l\right) \tag{14}$$

$$F_{iy} = F_{iy}^j + F_{iy}^l = \frac{1}{2}\sigma_y t\left(x_j - x_l\right) \tag{15}$$

Write the force vector of the four nodes in the matrix form

$$\mathbf{F}_x^e = \begin{bmatrix} F_{ix} \\ F_{jx} \\ F_{kx} \\ F_{lx} \end{bmatrix} = \frac{\sigma_x t}{2} \begin{bmatrix} 0 & 1 & 0 & -1 \\ -1 & 0 & 1 & 0 \\ 0 & -1 & 0 & 1 \\ 1 & 0 & -1 & 0 \end{bmatrix} \begin{bmatrix} y_i \\ y_j \\ y_k \\ y_l \end{bmatrix} = \frac{\sigma_x t}{2} \mathbf{A} \cdot \mathbf{y}^e \tag{16}$$

$$\mathbf{F}_y^e = \begin{bmatrix} F_{iy} \\ F_{jy} \\ F_{ky} \\ F_{ly} \end{bmatrix} = -\frac{\sigma_y t}{2} \begin{bmatrix} 0 & 1 & 0 & -1 \\ -1 & 0 & 1 & 0 \\ 0 & -1 & 0 & 1 \\ 1 & 0 & -1 & 0 \end{bmatrix} \begin{bmatrix} x_i \\ x_j \\ x_k \\ x_l \end{bmatrix} = -\frac{\sigma_y t}{2} \mathbf{A} \cdot \mathbf{x}^e \tag{17}$$

According to the equilibrium conditions at nodes shown in Fig. 4, the force equilibrium equations at node $i$ are

$$F_{ix} = -T_{ij}\frac{x_j - x_i}{L_{ij}} - T_{li}\frac{x_l - x_i}{L_{li}} = q_{ij}\left(x_i - x_j\right) + q_{li}\left(x_i - x_l\right) \tag{18}$$

$$F_{iy} = -T_{ij}\frac{y_j - y_i}{L_{ij}} - T_{li}\frac{y_l - y_i}{L_{li}} = q_{ij}\left(y_i - y_j\right) + q_{li}\left(y_i - y_l\right) \tag{19}$$

The force equilibrium equations on the four nodes can be written in the form of matrix as below

$$\mathbf{F}_x^e = \begin{bmatrix} x_i - x_j & 0 & 0 & x_i - x_l \\ x_j - x_i & x_j - x_k & 0 & 0 \\ 0 & x_k - x_j & x_k - x_l & 0 \\ 0 & 0 & x_l - x_k & x_l - x_i \end{bmatrix} \begin{bmatrix} q_{ij} \\ q_{jk} \\ q_{kl} \\ q_{li} \end{bmatrix} = \mathbf{X} \cdot \mathbf{q}^e \tag{20}$$

$$\mathbf{F}_y^e = \begin{bmatrix} y_i - y_j & 0 & 0 & y_i - y_l \\ y_j - y_i & y_j - y_k & 0 & 0 \\ 0 & y_k - y_j & y_k - y_l & 0 \\ 0 & 0 & y_l - y_k & y_l - y_i \end{bmatrix} \begin{bmatrix} q_{ij} \\ q_{jk} \\ q_{kl} \\ q_{li} \end{bmatrix} = \mathbf{Y} \cdot \mathbf{q}^e \tag{21}$$

Let $\mathbf{B}=[\mathbf{X}\ \mathbf{Y}]^T$, then

$$\mathbf{B} \cdot \mathbf{q}^e = \begin{bmatrix} \mathbf{F}_x^e \\ \mathbf{F}_y^e \end{bmatrix} = \frac{t}{2} \begin{bmatrix} \sigma_x \mathbf{A} & 0 \\ 0 & -\sigma_y \mathbf{A} \end{bmatrix} \begin{bmatrix} \mathbf{y}^e \\ \mathbf{x}^e \end{bmatrix} \tag{22}$$

Hence

$$\mathbf{q}^e = \frac{t}{2}\left(\mathbf{B}^T\mathbf{B}\right)^{-1}\mathbf{B}^T \begin{bmatrix} \sigma_x \mathbf{A} & 0 \\ 0 & -\sigma_y \mathbf{A} \end{bmatrix} \begin{bmatrix} \mathbf{y}^e \\ \mathbf{x}^e \end{bmatrix} \tag{23}$$

Then the force densities of the total members $\mathbf{q}$ can be obtained by adding element force densities $\mathbf{q}^e$ together

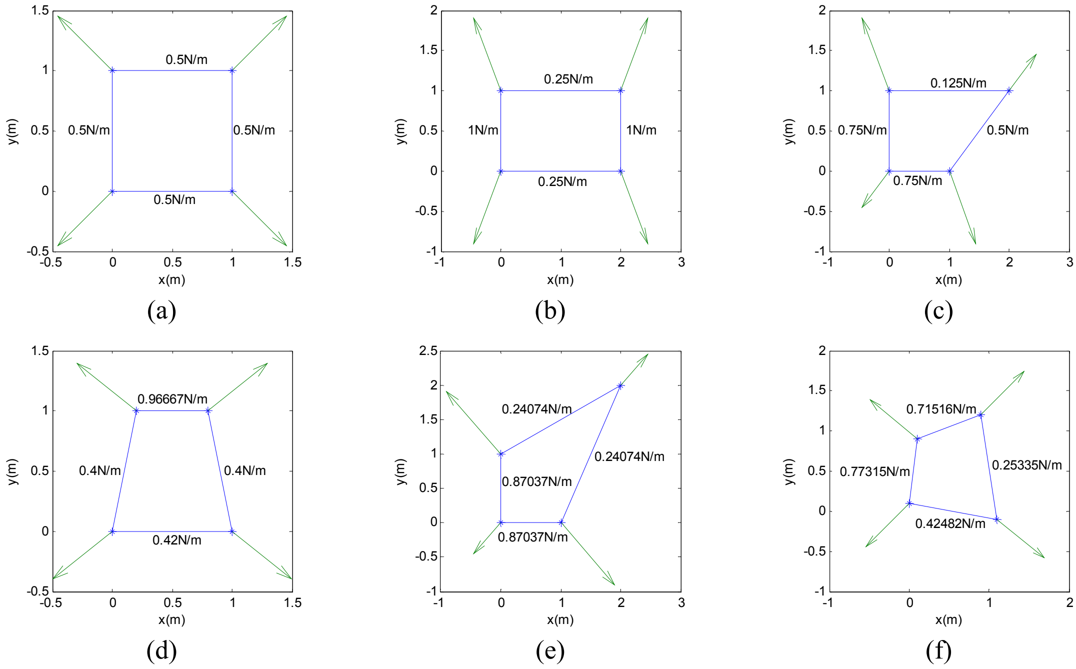


Fig. 5 Transform from element stresses to cable forces

$$\mathbf{q} \leftarrow \sum_{e} \mathbf{q}^{e} \tag{24}$$

From Eq. (23), one can assume that the transform relationship is depending on the coordinates of the nodes. Hence, in the form-finding process, the force density should be updated in every iterating step.

## 4. Numerical examples

### *4.1 Transform from element stresses to cable forces*

In order to verify the equivalent transforms relationship between force-densities of cable nets and the stresses of membrane elements, we take a single quadrangle element as an example. Suppose the element stress is $\sigma_x=\sigma_y=1$ kPa, $\sigma_{xy}=0$ kPa. The thickness of the element $t=1$ mm. Fig. 5 shows the equilibrium force densities of the cable segments in six different cases.

### *4.2 Form finding of a plane membrane*

A plane membrane structure fixed at the vertices of a square, with the length 10 m and the thickness 1 mm, is considered here. Fig. 6(a) shows its initially assumed shape and mesh. The initial stresses in the membrane are $\sigma_x=\sigma_y=1$ MPa and the initial force on the boundary cable is $T$=5 kN.

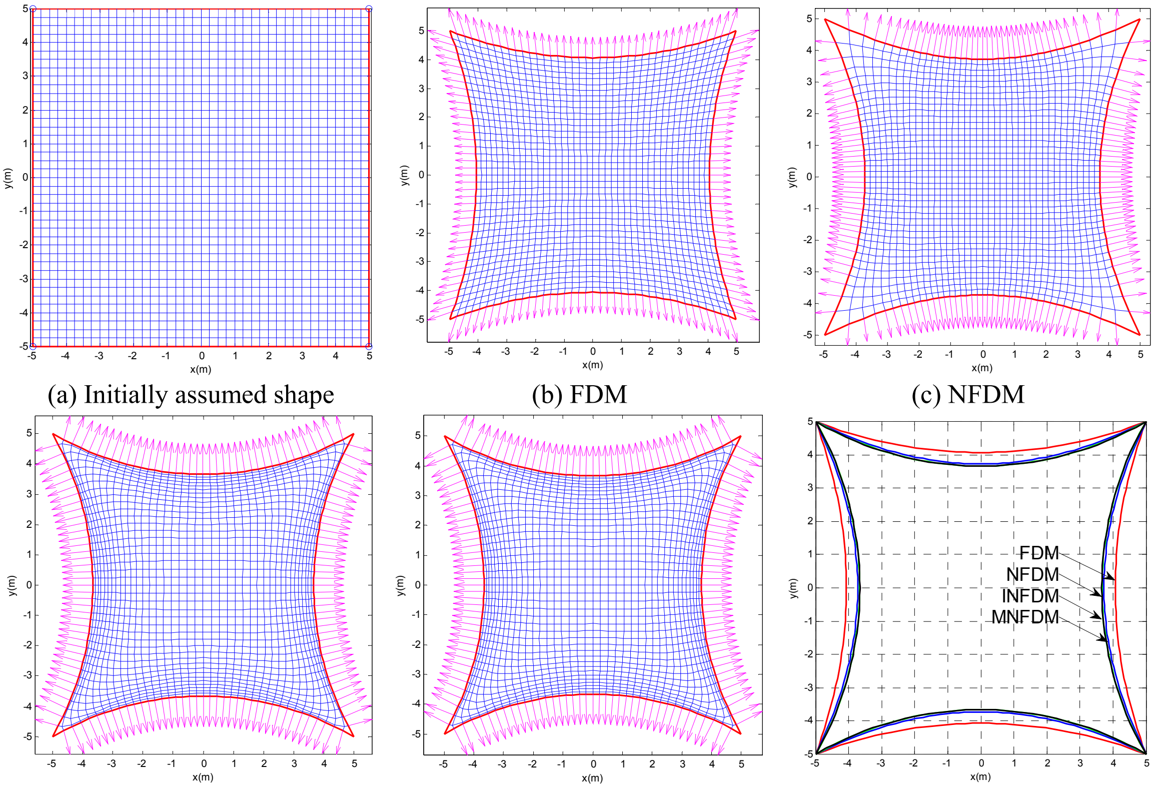


(a) Initially assumed shape (b) FDM (c) NFDM

(d) INFDM (e) MNFDM (f) Comparison

Fig. 6 Transform from element stresses to cable forces

The FDM, NFDM, INFDM and MNFDM are used to solve this problem respectively. For fair comparison, all methods are applied iteratively with 25 iterations. And the final viable shapes are shown in Fig. 6(b)-(e). Fig. 6(f) shows the comparison of the final shapes solved by these four methods. In Fig. 6(b)-(e), the red arrows stand for the tension force distribution of the boundary cable. The tension force of the boundary cable can be decompose into two parts: the normal force (vertical to the boundary cable curve) and the tangential force (tangent to the boundary cable curve), and they are compared in Fig. 7(a) and Fig. 7(b). As the initial stress of the membrane is set to 1 MPa, the normal force of the boundary cable would be 1 kN/m in the ideal case. Actually, the results demonstrate that the tension force solve by FDM is much less than 1 kN/m. That is because it did not consider the variety of the cable member length, the tension force go down with decreasing cable length while the force density is constant. By considering the variety of the cable member length, the tension force in the center solved by NFDM is much bigger than FDM. But the tension force in the corner becomes smaller, that's because the mesh in there becomes wider. The INFDM taking into account both the variety of the cable length and mesh width, it did improve the result significantly. However, the tension force distribution is still non-uniform. As the force densities are corrected by multiple the cable length and mesh width in INFDM. The correction method will be inaccurate while the mesh is seriously distorted. Hence, we can see the tension force solve by INFDM is decreasing in the two ends of the edged. In the MNFDM presented in this paper, the force densities are transformed from the initial membrane stresses through the

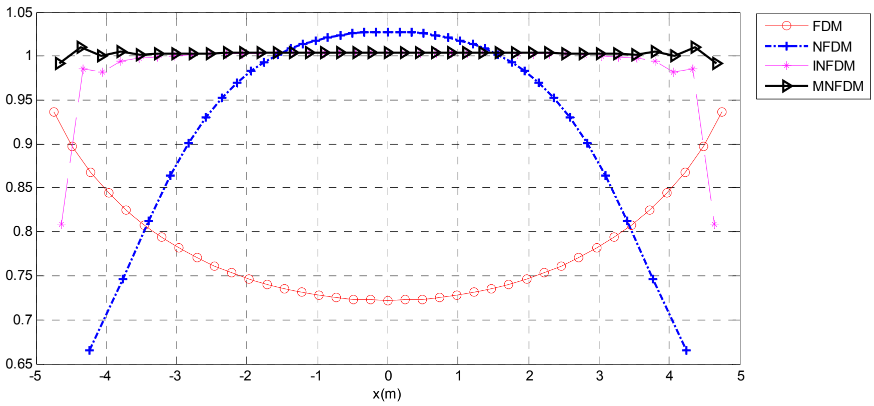


(a) Tension force

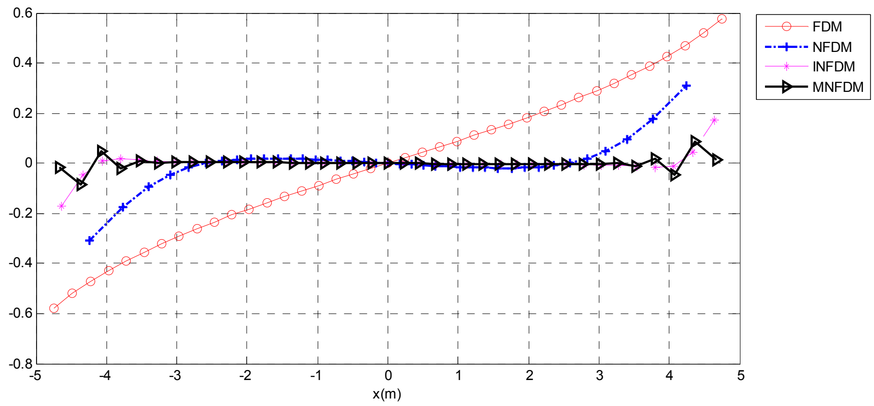


(b) Tangential force

Fig. 7 Tension and tangential force distribution comparison of the plane membrane

Table 1 Statistical index of normal force distribution of the plane membrane

| Method | Max | Min | Mean | STD | SSE |
|---|---|---|---|---|---|
| FDM | 0.9366 | 0.7221 | 0.7822 | 0.0629 | 1.9997 |
| NFDM | 1.0279 | 0.6649 | 0.9487 | 0.1029 | 0.5047 |
| INFDM | 1.0039 | 0.8091 | 0.9902 | 0.0431 | 0.0744 |
| MNFDM | 1.0103 | 0.9917 | 1.0032 | 0.0032 | 0.0008 |

equivalent transform relationship. Furthermore, by this method, the distribution of the tension force is expected to be very uniform.

Table 1 list the statistical index of tension force distribution solved by the four methods, which are maximum (Max), minimum (Min), mean, standard deviation (STD) and sum of squares of errors (SSE). It shows that the mean of the tension force distribution solved by MNFDM is 1.0032, it is the most approximate one to the ideal result.

Fig. 8 illustrates the length variations of the member in $x$-directions, and the statistical indexes are listed in Table 2. Several properties can be seen from the results:

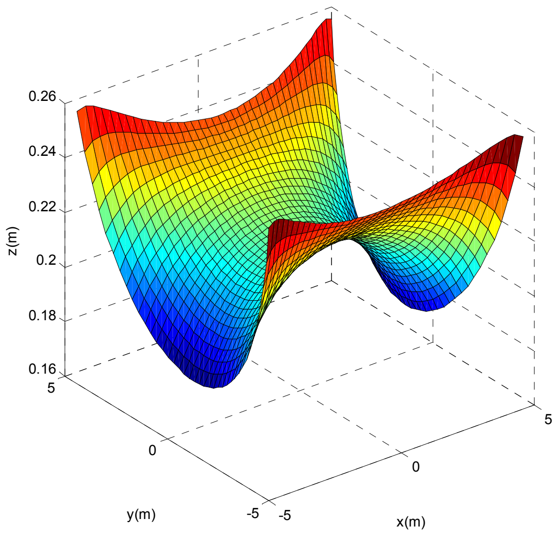


(a) FDM

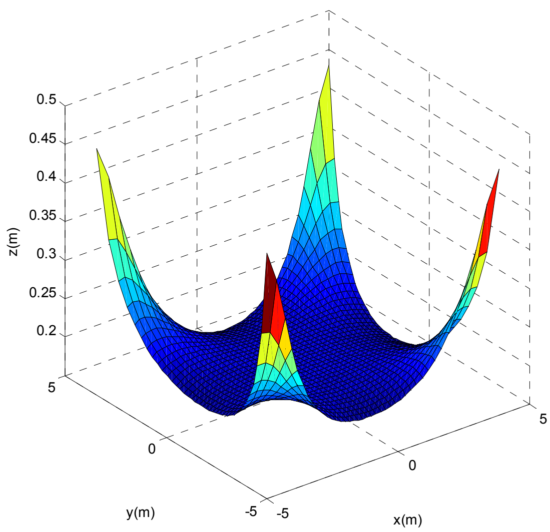


(b) NFDM

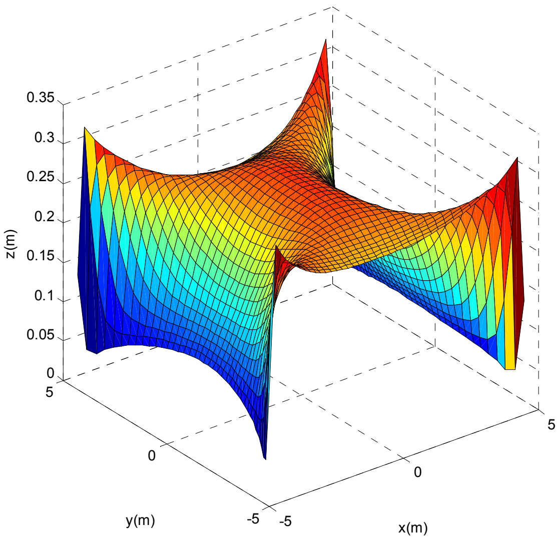


(c) INFDM

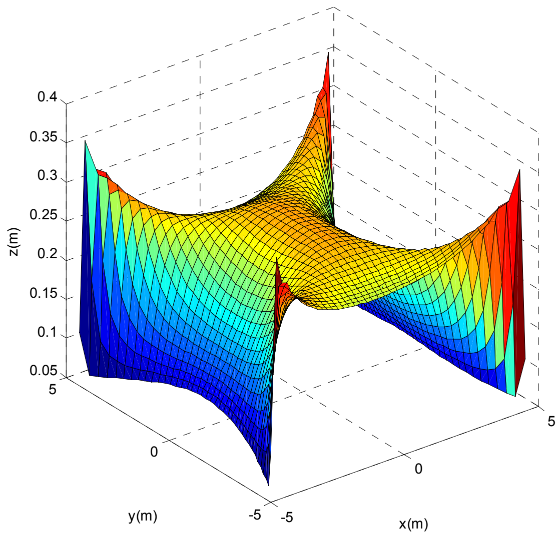


(d) MNFDM

Fig. 8 Length variations of the member in *x*-direction

Table 2 Statistical index of length variations of the member in x-direction

| Method | Max | Min | Max/Min | Mean | STD |
|---|---|---|---|---|---|
| FDM | 0.2591 | 0.1773 | 1.4614 | 0.2191 | 0.0173 |
| NFDM | 0.4497 | 0.1724 | 2.6085 | 0.1994 | 0.0291 |
| INFDM | 0.3212 | 0.0419 | 7.6659 | 0.2036 | 0.0644 |
| MNFDM | 0.3531 | 0.0577 | 6.1196 | 0.2036 | 0.0642 |

(1) For FDM, the member length of the left and right side are shortened, and the up and down side are lengthened;

(2) For NFDM, the member length of the four corner are lengthened, and center are shortened slightly;

(3) For INFDM and MNFDM, the member length variations are very similar: the left and right sides are shortened sharply, and the centers are lengthened slightly.

Since the problem of a plane membrane fixed at four points was considered as a benchmark, Pauletti and Pimenta (2008) present several border configurations for different tension force ($T$=100, 10, 5, 2, 1.5 and 1.41 kN) on the border cables, and discussed the solution from a theoretical point of view. Fig. 9 compares six different solutions for this problem solved by INFDM and NFDM. It is shown that the result of the two methods is much approximate to each other.

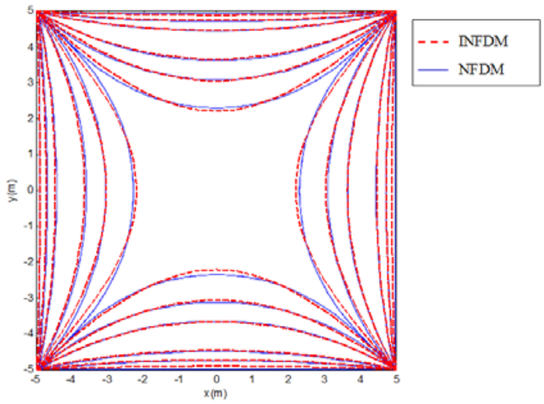


Fig. 9 Comparison of INFDM and NFDM under different tension force

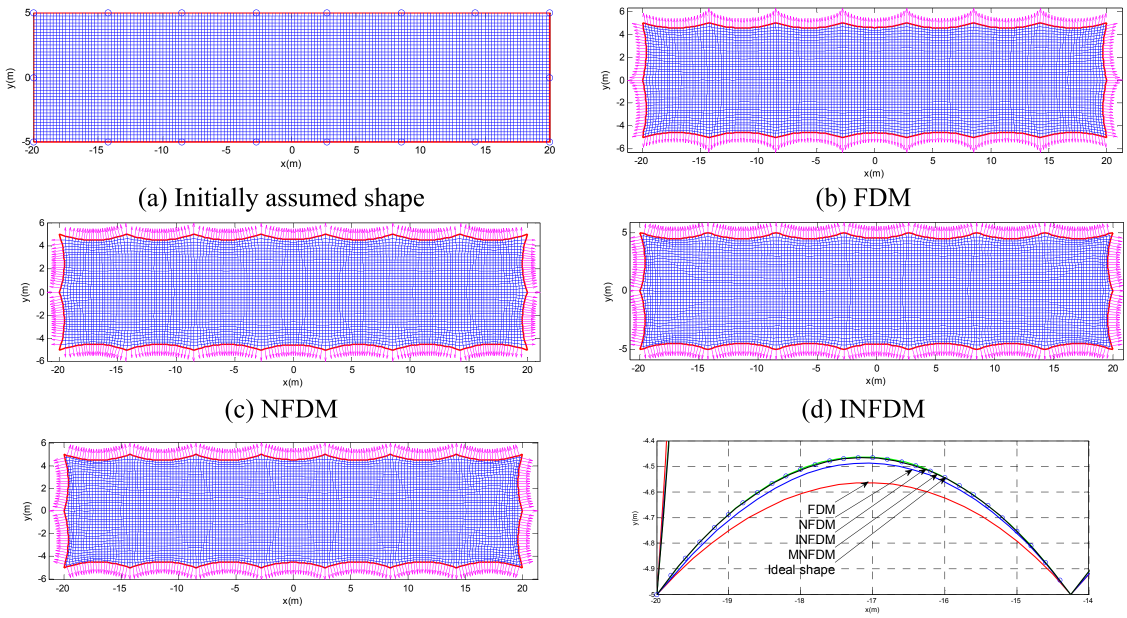


(a) Initially assumed shape (b) FDM

(c) NFDM (d) INFDM

(e) MNFDM (f) Comparison

Fig. 10 Form finding result of the membrane SAR antenna

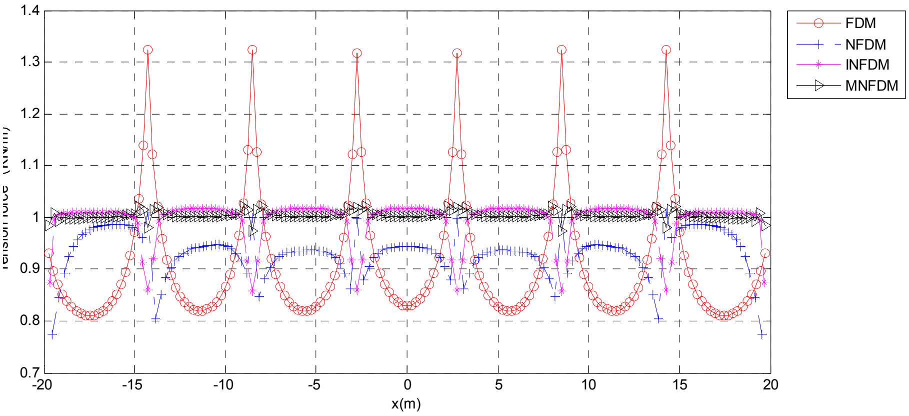


(a) Tension force

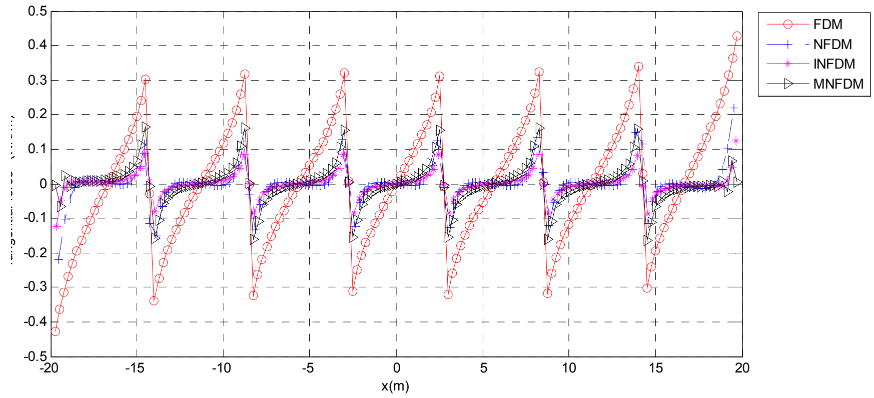


(b) Tangential force

Fig. 11 Tension force distribution comparison of the membrane SAR antenna

Table 3 Statistical index of normal force distribution of the membrane SAR antenna

| Method | Max | Min | Mean | STD | SSE |
|---|---|---|---|---|---|
| FDM | 1.3248 | 0.8096 | 0.9129 | 0.1209 | 3.5151 |
| NFDM | 1.0109 | 0.7742 | 0.9341 | 0.0420 | 0.9696 |
| INFDM | 1.0174 | 0.8571 | 0.9961 | 0.0400 | 0.2554 |
| MNFDM | 1.0205 | 0.9737 | 1.0038 | 0.0080 | 0.0123 |

### *4.3 Form finding of the membrane SAR antenna*

A membrane SAR antenna structure fixed at the 18 points of the edges, with width 10 m, length 40*m* and thickness 1 mm, is considered here. Its initial shape and mesh are presented in Fig. 10(a). The initial stresses in the membrane are $\sigma_x$=$\sigma_y$=1 MPa and the initial force on the boundary cable is $T$=8 kN. Fig. 10(b)-(e) illustrates the final viable shapes of the membranes solved by FDM, NFDM, INFDM and MNFDM, respectively. As the ideal shape of the border cables is known a priori as circular arches, if the membrane stress is homogeneous isotropic and the cable force is uniform normal. The four border configurations for different methods and the ideal shape are part enlarged and compared in Fig. 10(f). The red arrows in the figures stand for the tension force at the of the boundary cable. The tension force of the boundary cable can be decompose into two parts: the normal force (vertical to the boundary cable curve) and the tangential force (tangent to the boundary cable curve), and they are compared in Fig. 11(a) and (b). The results demonstrate that all the four tension force distribution and tangential force distribution are periodically changing.

Statistical indexes of tension force distribution are compared in Table 3. It is shown that the STD of the MNFDM is 0.008, which is much lesser than the other three methods. Moreover, the mean and SSE of the tension force distribution solved by MNFDM is 0.0123. As in theoretical, the normal force distribution and the tangent force distribution are 1 kN/m and 0 kN/m, respectively. Therefore, we can demonstrate that the result of MNFDM is the most approximate one to the theoretical result.

## 5. Conclusions

This paper addressed the form-finding problem of cable-membrane structures. Attempting to find a viable initial configuration with a uniform, isotropic plane stress state for the cable-membrane structures, an equivalent transformation relationship between force-densities of cable nets and the stresses of membrane elements was established. Based on such relationship, a modified nonlinear force density method (MNFDM) was proposed. Numerical examples are conducted to verify the proposed method and the following conclusions can be drawn:

• The membrane stress and cable tension are used as initial conditions instead of assuming the value of force density, this would avoid the complicated trial calculation process and makes the process of form-finding more concise, efficient and clear.

• The MNFDM is more accurate than FDM, NFDM and INFDM in the same iterations. In the present simulation cases, the final shapes solved by it have a very uniform stresses distribution. The max errors of the edge normal force are less than 2.05% in both cases. These results are much appropriate to the theoretical one.

## References

Barnes, M.R. (1999), "Form-finding and analysis of tension structures by dynamic relaxation", *Int. J. Space Struct.*, **14**(2), 89-104.

Bradshaw, R., Campbell, D., Gargari, M., Mirmiran, A. and Tripeny, P. (2002), "Special structures: past, present, and future", *J. Struct. Eng.*, ASCE, **128**(6), 691-709.

Colinas, J., Potvin, M.J., Jiang, X.X., Girard, R., Geneviève, T. and Cascarano, B. (2005), "Recent developments on C-band membrane antennas for small -sat SAR at the canadian space agency", *28th ESA Antenna Workshop on Space Antenna Systems and Technologies*, Noordwijk, Netherlands, May.

Grahne, M. and Cadogan, D. (1999), "Inflatable solar arrays: revolutionary technology? ", *SAE Technical Paper*, **01**, 2551.

Greco, L. and Cuomo, M. (2012), "On the force density method for slack cable nets", *Int. J. Solid. Struct.*, **49**(13), 1526-1540.

Hernandez-Montes, E., Jurado-Pina, R. and Bayo, E. (2006), "Topological mapping for tension structures", *J. Struct. Eng.*, ASCE, **132**(6), 970-977.

Lane, S.A., Murphey, T.W. and Zatman, M. (2011), "Overview of the Innovative Space-Based Radar

Antenna Technology Program", *J. Spacecraft Rock.*, **48**(1), 135-145.
Leifer, J., Jones, D.C. and Cook, A.M. (2010), "Gravity-Induced Wrinkling in Subscale, Singly Curved Parabolic Gossamer Membrane", *J. Spacecraft Rock.*, **47**(1), 214-219.
Linkwitz, K. (1971), "New methods for the determination of cutting pattern of prestressed cable nets and their application to the olympic roofs munich", *Proceedings of the IASS Pacific Symposium on Tension Structures and Space Frames*, Tokyo.
Linkwitz, K. and Schek, H.J. (1971), "Einige Bemerkungen zur Berechnung von vorgespannten Seilnetzkonstruktionen", *Ingenieur-Archiv.*, **40**, 145-158.
Liu, W. and Li, D.X. (2013a), "Simple Technique for Form-Finding and Tension Determining of Cable-Network Antenna Reflectors", *J. Spacecraft Rock.*, **50**(2), 479-481.
Liu, W., Li, D.X. and Jiang, J.P. (2013b), "Mesh topological form design and geometrical configuration generation for cable-network antenna reflector structures", *Struct. Eng. Mech.*, **45**(3), 411-422.
Liu, W., Li, D.X. and Jiang, J.P. (2013c), "General Mesh Configuration Design Approach for Large Cable-Network Antenna Reflectors", *J. Struct. Eng.*, ASCE, **140**(2),04013051.
Maurin, B. and Motro, R. (1998), "The surface stress density method as a form-finding tool for tensile membranes", *Eng. Struct.*, **20**(8), 712-719.
Maurin, B. and Motro, R. (2004), "Concrete shells form-finding with surface stress density method", *J. Struct. Eng.*, ASCE, **130**(6), 961-968.
Morterolle, S., Maurin, B., Quirant, J. and Dupuy, C. (2012), "Numerical form-finding of geotensoid tension truss for mesh reflector", *Acta Astronaut*, **76**, 154-163.
Nouri-Baranger, T. (2004), "Computational methods for tension-loaded structures", *Arch. Comput. Meth. Eng.*, **11**, 143-186.
Pauletti, R.M.O. and Pimenta, P.M. (2008), "The natural force density method for the shape finding of taut structures", *Comput. Meth. Appl. Mech. Eng.*, **197**, 4419-4428.
Quagliaroli, M. and Malerba, P.G. (2013), "Flexible bridge decks suspended by cable nets. A constrained form finding approach", *Int. J. Solid. Struct.*, **50**(14-15), 2340-2352.
Schek, H.J. (1974), "The force density method for form finding and computations of general network", *Comput. Meth. Appl. Mech. Eng.*, **3**, 115-134.
Straubel, M., Langlois, S., Sinapius, M. and Hühne, C. (2010), "Simulation and test on mechanical behavior of a deployable membrane antenna", *32nd ESA Antenna Workshop*, Noordwijk, The Netherlands, October.
Tran, H.C. and Lee, J. (2013), "Force methods for trusses with elastic boundary conditions", *Int. J. Mech. Sci.*, **66**, 202-213.
Tsiatas, G.C. and Katsikadelis, J.T. (2006), "Large deflection analysis of elastic space membranes", *Int. J. Numer. Meth. Eng.*, **65**, 264-294.
Valdés, J.G., Miquel, J. and Oñate, E. (2009), "Nonlinear finite element analysis of orthotropic and prestressed membrane structures", *Finite Elem. Anal. Des.*, **45**(6-7), 395-405.
Veenendaal, D. and Block, P. (2012), "An overview and comparison of structural form finding methods for general networks", *Int. J. Solid. Struct.*, **49**, 3741-3753.
Xiang, X.A., Wei, T., Yang, Z. and Shi-lin, D. (2010), "Improved nonlinear force density method accounting for 2-dimensional deformations of membrane element", *Eng. Mech.*, **27**(4), 251-256.
Xu, X. and Luo, Y. (2011), "Multistable Tensegrity Structures", *J. Struct. Eng.*, ASCE, **137**(1), 117-123.
Ye, J.H., Feng, R.Q., Zhou, S.L. and Tian, J. (2012), "The modified force-density method for form-finding of membrane structures", *Int. J. Steel Struct.*, **12**(3), 299-310.
Zhang, L., Maurin, B. and Motro, R. (2006), "Form-finding of nonregular tensegrity systems", *J. Struct. Eng.*, ASCE, **132**(9), 1435-1440.
Zhang, Q.L., Chen, L.X. and Luo, X.Q. (2007), "Equivalent transform from the force-densities of cable net to the the stresses of membrane elements", *Struct. Eng. Mech.*, **26**(4), 479-482.

*CC*